

ACCEPTED MANUSCRIPT • OPEN ACCESS

Global hydrological models continue to overestimate river discharge

To cite this article before publication: Stefanie Heinicke *et al* 2024 *Environ. Res. Lett.* in press <https://doi.org/10.1088/1748-9326/ad52b0>

Manuscript version: Accepted Manuscript

Accepted Manuscript is “the version of the article accepted for publication including all changes made as a result of the peer review process, and which may also include the addition to the article by IOP Publishing of a header, an article ID, a cover sheet and/or an ‘Accepted Manuscript’ watermark, but excluding any other editing, typesetting or other changes made by IOP Publishing and/or its licensors”

This Accepted Manuscript is © 2024 The Author(s). Published by IOP Publishing Ltd.



As the Version of Record of this article is going to be / has been published on a gold open access basis under a CC BY 4.0 licence, this Accepted Manuscript is available for reuse under a CC BY 4.0 licence immediately.

Everyone is permitted to use all or part of the original content in this article, provided that they adhere to all the terms of the licence <https://creativecommons.org/licenses/by/4.0>

Although reasonable endeavours have been taken to obtain all necessary permissions from third parties to include their copyrighted content within this article, their full citation and copyright line may not be present in this Accepted Manuscript version. Before using any content from this article, please refer to the Version of Record on IOPscience once published for full citation and copyright details, as permissions may be required. All third party content is fully copyright protected and is not published on a gold open access basis under a CC BY licence, unless that is specifically stated in the figure caption in the Version of Record.

View the [article online](#) for updates and enhancements.

Global hydrological models continue to overestimate river discharge

Stefanie Heinicke^{1*}, Jan Volkholz^{1*}, Jacob Schewe¹, Simon Gosling², Hannes Müller Schmied^{3,4}, Sandra Zimmermann¹, Matthias Mengel¹, Inga Sauer¹, Peter Burek⁵, Jinfeng Chang⁶, Sian Kou-Giesbrecht⁷, Manoli Grillakis⁸, Luca Guillaumot^{5,9}, Naota Hanasaki¹⁰, Aristeidis Koutroulis⁸, Kedar Otta¹⁰, Wei Qi¹¹, Yusuke Satoh¹², Tobias Stacke¹³, Tokuta Yokohata¹⁰, Katja Frieler¹

¹ Potsdam Institute for Climate Impact Research (PIK), Member of the Leibniz Association, Potsdam, Germany

² School of Geography, Faculty of Social Sciences, University of Nottingham, Nottingham, United Kingdom

³ Institute of Physical Geography (IPG), Goethe-University Frankfurt, Frankfurt am Main, Germany

⁴ Senckenberg Leibniz Biodiversity and Climate Research Centre (SBIK-F), Frankfurt am Main, Germany

⁵ International Institute for Applied Systems Analysis, Laxenburg, Austria

⁶ College of Environmental and Resource Sciences, Zhejiang University, Zhejiang, China

⁷ Department of Earth and Environmental Sciences, Dalhousie University, Halifax, Canada

⁸ Technical University of Crete, Chania, Greece

⁹ Water, Environment, Processes and Analyses Division, BRGM – French Geological Survey, Orléans, France

¹⁰ National Institute for Environmental Studies, Tsukuba, Japan

¹¹ Southern University of Science and Technology, China

¹² Korea Advanced Institute of Science and Technology (KAIST), Daejeon, Republic of Korea

¹³ Max Planck Institute for Meteorology, Germany

*shared first author

E-mail: heinicke@pik-potsdam.de

Keywords: model evaluation, model intercomparison, flood, hydrological extremes, river routing

Abstract

Global hydrological models (GHMs) are widely used to assess the impact of climate change on streamflow, floods, and hydrological droughts. For the ‘model evaluation and impact attribution’ part of the current round of the Inter-Sectoral Impact Model Intercomparison Project (ISIMIP3a), modelling teams generated historical simulations based on observed climate and direct human forcings with updated model versions. Here we provide a comprehensive evaluation of daily and maximum annual discharge based on ISIMIP3a simulations from nine GHMs by comparing the simulations to observational data from 644 river

1
2
3 gauge stations. We also assess low flows and the effects of different river routing schemes. We find that
4 models can reproduce variability in daily and maximum annual discharge, but tend to overestimate both
5 quantities, as well as low flows. Models perform better at stations in wetter areas and at lower elevations.
6
7 Discharge routed with the river routing model CaMa-Flood can improve the performance of some models,
8 but for others, variability is overestimated, leading to reduced model performance. This study indicates that
9 areas for future model development include improving the simulation of processes in arid regions and cold
10 dynamics at high elevations. We further suggest that studies attributing observed changes in discharge to
11 historical climate change using the current model ensemble will be most meaningful in humid areas, at low
12 elevations, and in places with a regular seasonal discharge as these are the regions where the underlying
13 dynamics seem to be best represented.
14
15
16
17
18
19
20
21
22
23
24

25 **1 Introduction**

26 The water cycle is particularly susceptible to climate change, leading to changes in river flow with far-
27 reaching consequences for water availability for humans (e.g., hydrological droughts), for climatic hazards
28 such as river floods, but also for ecosystems (Gudmundsson *et al* 2021, Maxwell *et al* 2019, Schewe *et al*
29 2014, Thompson *et al* 2021, Van Mliet 2023). Fluvial floods led to the death of more than 200,000 people
30 and incurred damages of 790 billion USD from 1980 to 2016 (Munich Re 2016). In addition, it has been
31 estimated that floods and droughts resulted in 25 million people living in extreme poverty (Hallegatte *et al*
32 2017). Model-based projections show a strong increase in land area and population exposed to river floods
33 and droughts due to increased global warming (Lange *et al* 2020).
34
35
36
37
38
39
40
41
42
43

44 Hydrological models are an important tool for decision-making in flood and drought management and
45 preparedness and are used to make projections under different climate, land-use, and management
46 scenarios. Global hydrological models (GHMs) in particular have been used, for example, to assess the
47 impact of global warming on the availability of water resources (Pokhrel *et al* 2021, Schewe *et al* 2014, Liu
48 *et al* 2017a), and on flood hazards (Dankers *et al* 2014, Hirabayashi *et al* 2021). In addition, GHMs can be
49 used to attribute changes in the hydrological system to climate change. For example, Gudmundsson *et al*
50
51
52
53
54
55
56
57
58
59
60

1
2
3 (2021) showed that observed changes in river flow are consistent with climatic changes, and Sauer et al
4
5 (2021) found a climate signal in the trends in damages caused by river floods.
6

7 The evaluation of hydrological models is a critical first step towards impact attribution and future
8 projections as for both purposes we need to understand to what degree models capture the processes
9 determining discharge at individual locations, regions or globally. To this end, GHMs have been forced by
10 observational climate data and observational direct human forcings (e.g., land use, location of dams and
11 reservoirs) in ISIMIP2 already. These previous ISIMIP2 simulations have been evaluated, for example,
12 regarding the influence of river routing on simulated discharge (Zhao *et al* 2017), the incorporation of
13 human impact parameterizations (Liu *et al* 2017b, Veldkamp *et al* 2018), drought characteristics (Kumar
14 *et al* 2022), or the seasonality of mean and extreme runoff (Zaherpour *et al* 2018). It has been shown that
15 GHMs can simulate the extent of flooded areas, but for some events, GHMs overestimate the flood extent
16 (Mester *et al* 2021). In addition, studies on economic damages caused by river floods showed that
17 interannual variability of observed damages can be captured at least in some large scale areas (Sauer *et al*
18 2021). Deviations at the damage level could be due to either the discharge simulated by GHMs or from
19 other sources in the modelling chain (e.g., assumed river protection levels, estimated distribution of assets,
20 local physical vulnerabilities, Sauer *et al* 2021).
21
22
23
24
25
26
27
28
29
30
31
32
33
34
35

36 For ISIMIP3a, the climate input data and information on direct human forcings have been updated. For
37 example, the data cover three additional years (2017-2019), accordingly more recent observational data has
38 been used for bias adjustment, and an update in the bias adjustment method reduced excessively high daily
39 maximum temperature values (Lange *et al* 2021, table 1 in Frieler *et al* 2024 shows details on data provided
40 for daily climate, land use, irrigation, dams and reservoirs, and water abstraction). This study
41 comprehensively evaluates the performance of nine global hydrological models that have contributed
42 discharge data to ISIMIP3a so far. Five of these models were updated in terms of improving the
43 representation of hydrological processes, and three models improved the representation of land cover
44 (details in table 1). The effect of these improvements has been evaluated elsewhere (Müller Schmied *et al*
45 2023, Tsilimigkras *et al* 2023, Boulange *et al* 2023, Yoshida *et al* 2022).
46
47
48
49
50
51
52
53
54
55
56
57
58
59
60

Table 1. Model improvements implemented since ISIMIP2a for models evaluated in this study. More details on models in table S1.

Model	hydrological processes	land-cover representation	comment	Reference
CLASSIC			did not participate in ISIMIP2a	Melton et al., 2020
CWatM	change in calculation of evapotranspiration with Penman-Monteith using CO ₂ response of vegetation	using time varying land use instead of static		Burek et al., 2020
H08	land surface model parameters have been optimized at each climatic zone			Boulangue <i>et al</i> 2023, Yoshida <i>et al</i> 2022
HydroPy			did not participate in ISIMIP2, model was rewritten based on MPI-HM which did participate in ISIMIP2, changes in model infrastructure, numerics and documentation	Stacke & Hagemann, 2021
JULES-W2	1) snow process module upgraded to 10-layer scheme; 2) soil hydrology scheme was changed to TOPMODEL scheme	1) plant functional type (PFT) representation was changed from 5 PFTs to 13 PFTs, 2) used time varying land use instead of static		Tsilimigkras et al under review, Best et al 2011
MIROC-INTEG-LAND			same as ISIMIP2a	Yokohata et al., 2020
ORCHIDEE-MICT	improvements for high-latitude processes including snow and permafrost, specifically 1) soil freezing and snow processes; 2)			Guimberteau et al 2018

1
2
3
4
5
6
7
8
9
10
11
12
13
14
15
16
17
18
19
20
21
22
23
24
25
26
27
28
29
30
31
32
33
34
35
36
37
38
39
40
41
42
43
44
45
46
47

	soil hydrology and river routing; 3) soil carbon discretization and SOM-dependent soil thermal and hydraulic parameters for permafrost representation; 4) reformulation of soil hydric stress above the permafrost table; 5) fires			
WaterGAP2-2e	updated input for sectoral water use models, updated and extended data base for calibration, modified calibration routine to consider observation uncertainty; storage-based river velocity algorithm; updated input for surface water bodies (e.g. GRanD 1.3), implemented river water temperature, diverse corrections in water abstraction procedure			Müller Schmied et al., 2021, 2023
WEB-DHM-SG		used time varying land use instead of static		Qi et al., 2022

1
2
3 The aim of this study is to intercompare model performance regarding daily and maximum annual
4 discharge as well as low flow and compare the performance of the models' internal routing schemes to
5 discharge generated from runoff by CaMa-Flood (Yamazaki *et al* 2011). We investigate which catchment
6 properties correlate with model performance to suggest areas of model development and to identify stations
7 that are particularly suitable for potential attribution studies or assessments of changes under future global
8 warming as considered in ISIMIP3.
9
10
11
12
13
14
15

16 17 **2 Methods**

18 19 *2.1 Simulated runoff and river discharge*

20
21 We use daily runoff and river discharge provided by nine modelling groups based on the ISIMIP3a
22 simulation round (Frieler *et al* 2024): CLASSIC, CWatM, H08, HydroPy, JULES-W2, MIROC-INTEG-
23 LAND, ORCHIDEE-MICT, WaterGAP2-2e, and WEB-DHM-SG (table S1). WaterGAP2-2e is calibrated
24 with observed discharge data (Müller Schmied *et al* 2023), and H08 uses parameters optimized to reproduce
25 observed discharge in each climatic zone (Yoshida *et al* 2022). Simulated data are from the
26 'obsclim + histsoc' experiment that is designed for model evaluation and uses observation-based daily
27 atmospheric climate forcing (GSWP3-W5E5, Lange *et al* 2023) and varying direct human forcings
28 provided by ISIMIP (Frieler *et al* 2024). According to ISIMIP model documentation (www.isimip.org), all
29 GHMs use land-use data, five models use data on water-use (CWatM, H08, HydroPy, MIROC-INTEG-
30 LAND, WaterGAP2-2e) and four models use data on dams and reservoir (CWatM, H08, MIROC-INTEG-
31 LAND, WaterGAP2-2e). Simulations are done on a 0.5°x0.5° grid and are available for the years 1901–
32 2019.
33
34
35
36
37
38
39
40
41
42
43
44
45

46 It has been shown that modelled peak river discharge using the river routing model CaMa-Flood
47 (Yamazaki *et al* 2011) can perform better than the model's internal routing scheme (Zhao *et al* 2017).
48 CaMa-Flood differs from other routing schemes in that it explicitly also parameterizes flood inundation
49 dynamics and provides water depth and inundation extent as output variables (Yamazaki *et al* 2011). It is
50 therefore often used in combination with GHMs for flood modelling. CaMa-Flood provides its own routing
51
52
53
54
55
56
57
58
59
60

1
2
3 scheme on a 15' grid. However, CaMa-Flood does not include the lakes and reservoirs routines simulated
4 by GHMs, which can result in some models performing better without CaMa-Flood. Thus, in addition to
5 discharge routed with each model's internal routing scheme (specified in table S1), we use each model's
6 simulated runoff to drive CaMa-Flood and then derive river discharge. Daily runoff is provided by all nine
7 models listed above, and discharge modelled with the model's internal routing scheme is provided by seven
8 models. JULES-W2 provides discharge routed with the 'native JULES' river topography (Total Runoff
9 Integrating Pathways scheme (TRIP)) that includes spatially distributed meandering and velocity data
10 (Tsilimigkras *et al* 2023), and has been shown to improve the accuracy of river flow simulations
11 (Tsilimigkras *et al* under review). In addition, JULES-W2 provides discharge routed with the DDM30 river
12 topology.

23 24 25 *2.2 Station selection and observed discharge data*

26 To evaluate model performance, we use daily discharge data from the Global Runoff Data Centre
27 (GRDC). GHMs use different river routing schemes (detailed in Table S1) and the spatial coordinates of
28 stations with observational data often do not match the coarser gridded river networks (Müller Schmied and
29 Schiebener 2022). To ensure comparability, we base the selection of stations on a previously published
30 report that analysed how well ISIMIP GHMs' routing schemes align with the location of a selection of
31 GRDC stations and are thus suitable for evaluating river discharge (Müller Schmied and Schiebener 2022).
32 1096 out of 1509 stations were found to be compatible (Müller Schmied and Schiebener 2022). Of those,
33 we select stations for which daily data was available for at least five years, and we only retain years with
34 less than ten days of missing data, which are the same criteria as used by Zhao *et al.* (2017). In the end, we
35 use 644 stations for model evaluation (figure 1), corresponding to 106 basins according to HydroBASINS
36 level 3 from the HydroSHEDS database (figure S1, Lehner and Grill 2013).

37 38 39 *2.3 Model evaluation*

40 We analyse the extent to which model simulations can reproduce variability in daily discharge and
41 maximum annual discharge. For both these metrics, and for each station and each GHM, we compare
42
43
44
45
46
47
48
49
50
51
52
53
54
55
56
57
58
59
60

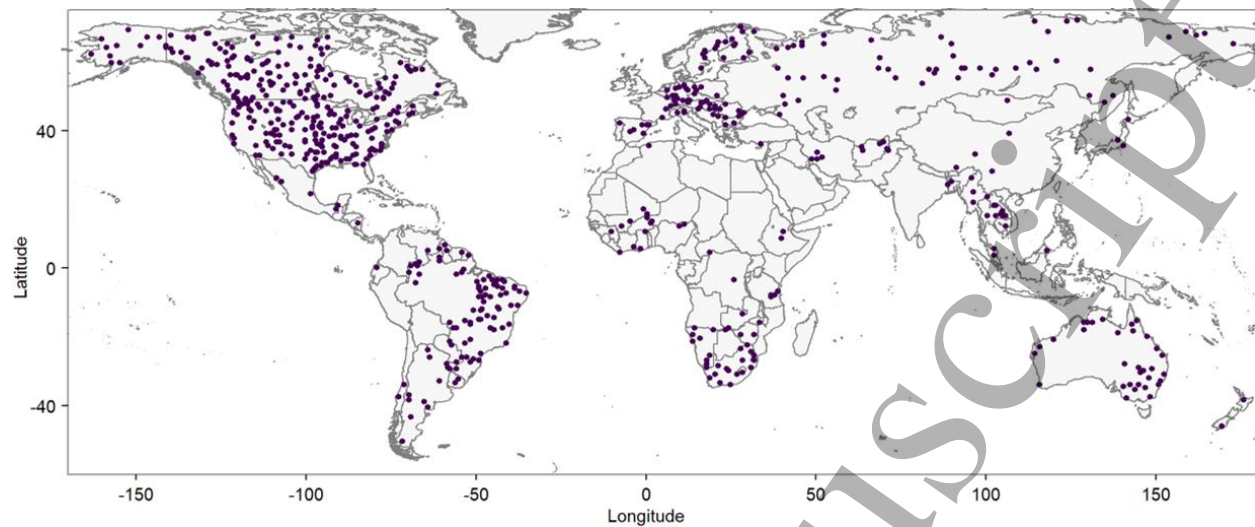


Figure 1. The location of the 644 GRDC stations used for model evaluation.

observed discharge to discharge routed with the model's internal routing scheme, and discharge routed with CaMa-Flood, respectively. To evaluate model performance, we calculate the Kling–Gupta efficiency (KGE) and its three components: correlation (r), bias ratio (β), and variability ratio (γ) (Kling *et al* 2012). The KGE is used to evaluate hydrological models (e.g., Veldkamp *et al* 2018, Krysanova *et al* 2017) and measures the ability of a model to reproduce observed values. It is calculated by equally weighing the three components, where r is the linear correlation between observed and simulated values, β is the ratio of the mean simulated value to the mean observed value, and γ is the ratio of the standard deviation of simulated values to the standard deviation of observed values (Knoben *et al* 2019). The KGE metric is dimensionless. We calculate the KGE for daily and maximum annual discharge for each model and each station.

For daily discharge, we also evaluate timing differences by testing whether shifting the simulated time series by up to 31 days (back- and forward) improves correlation, as has been suggested by Zhao *et al* (2017).

For maximum annual discharge, we quantify which part of the distribution is over- or underestimated. For each station, we first identify the lower 50% of observational values and count the years where the simulated values are lower or higher, and then we do the same for the upper 50% of observed values.

1
2
3 To assess the capability of models to simulate low flow, we first determine the tenth quantile of daily
4 discharge, i.e., the amount of discharge that is exceeded 90% of the time (Q90, Gosling *et al* 2017,
5 Krysanova *et al* 2017). We then divide the difference between simulated tenth percentile and observed tenth
6 percentile by observed tenth percentile. Thus, a value of zero implies a perfect match between observation
7 and simulation, negative values imply that the simulated low flow is too low, while positive values indicate
8 that the simulated low flow is simulated as too high. This is implemented for discharge routed with the
9 model's internal routing scheme, and discharge routed with CaMa-Flood.
10
11
12
13
14
15
16
17

18 To depict spatial heterogeneity in model performance, we calculated for each model the mean low flow
19 index and mean KGE for maximum annual discharge for each of the 106 basins (figure S1, Lehner and
20 Grill 2013).
21
22
23
24

25 *2.4 Station characteristics*

26 We use station characteristics data from the Global Streamflow Indices and Metadata Archive (GSIM)
27 that provides metadata for more than 30,000 stations (Do *et al* 2018, Gudmundsson *et al* 2018). GSIM data
28 is only available for a subset of stations in this study. We use the following catchment properties from the
29 database (number of stations with data available in parentheses): clay content (432), drainage density (379),
30 elevation (436), irrigated area [%] (436), nightlight development index (176), number of dams upstream
31 (436), population count (435), population density (435), sand content (432), silt content (433), slope (436),
32 storage volume (total upstream storage volume, 436), and topographic index (436). The upstream catchment
33 area from the gauge is taken from the GRDC database. To characterize how dry or wet the area is where a
34 station is located, we used data from the Global Aridity Index and Potential Evapotranspiration Database
35 (Zomer *et al* 2022). This aridity index is defined as the ratio of precipitation to potential evapotranspiration
36 and is unitless (Zomer *et al* 2022). Both, catchment area and aridity index are available for all stations.
37
38
39
40
41
42
43
44
45
46
47
48
49

50 To further investigate model performance at (sub-)arid stations, we first identified all stations with an
51 aridity index less than or equal to 0.5 (Zomer *et al* 2022). For these 236 stations, we calculated the KGE
52
53
54
55
56
57
58
59
60

1
2
3 and its three components for daily discharge, maximum and mean annual discharge, mean monthly and
4 long-term mean monthly discharge.
5
6

7 8 **3 Results** 9

10 **3.1 Daily discharge**

11 In general, models can reproduce the variability of daily river discharge at most stations (e.g., time-series
12 plot with corresponding KGE values in figure S2, S3). The median KGE across all stations ranges from -
13 0.43 for model WEB-DHM-SG to 0.46 for WaterGAP2-2e (figure 2a, table S2). The median correlation
14 ranges from 0.17 for the model CLASSIC to 0.68 for WaterGAP2-2e (figure 2b, table S2). Most models
15 (seven out of nine) tend to overestimate daily discharge at a majority of stations (bias ratio β larger than
16 one), but there is a large variation in the magnitude of overestimation between models, as well as between
17 stations (figure 2c, table S2). Results for the variability ratio (γ) are mixed, with two (out of nine) models
18 overestimating variability (e.g., HydroPy), while the remaining models tend to underestimate variability
19 (e.g., MIROC-INTEG-LAND, figure 2d, table S2).
20
21
22
23
24
25
26
27
28
29
30

31 Models tend to perform well at stations in wetter areas (i.e., higher aridity index, table S3, figure 3), and
32 less well at stations at higher elevations (table S3, figure 4), while in drier areas and at lower elevations
33 there is a large spread across stations including good and poor model performance. The bias ratio tends to
34 be larger at stations in drier areas (figure S4, table S5). For several models (six out of nine), the variability
35 ratio is larger at higher catchment elevations (table S6, figure S5) and steeper slopes (table S6, figure S6).
36 Stations for which models perform best (i.e., highest KGE and correlation across all models) are, for
37 example, located at the Mekong River in Southeast Asia, and the Amazon River in South America.
38
39
40
41
42
43
44
45

46 Shifting the time series can lead to improved correlation (figure S7), but the more shifting is required the
47 worse model performance of shifted time-series is (figure S8).
48
49

50 Regarding the use of river routing schemes, discharge routed with CaMa-Flood performs better for three
51 out of seven models, especially for ORCHIDEE-MICT and WEB-DHM-SG (figure 2a). For these cases,
52 KGE and especially its first component (correlation) is higher (figure 2a, 2b), but at the same time bias and
53
54
55
56
57
58
59
60

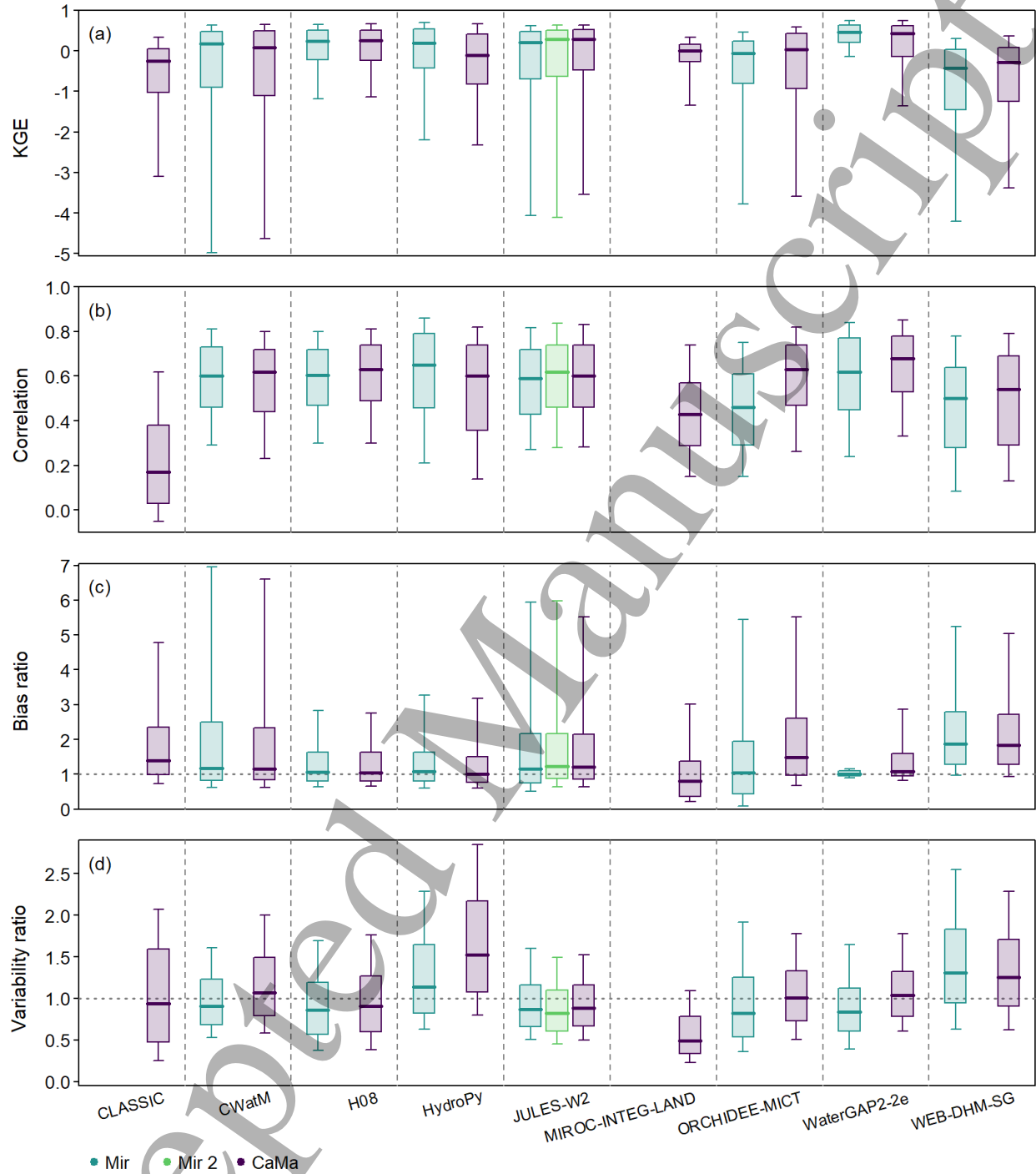


Figure 2. Evaluation of daily discharge routed by the model's internal routing scheme (Mir) and CaMa-Flood (CaMa) across 644 stations for Kling-Gupta efficiency (KGE) and its three components. JULES-W2 provides discharge routed with two routing schemes (Mir, Mir2, details in table S1). Thick lines: median, box: first and third quartile, whiskers: 10th and 90th percentile. Details table S2.

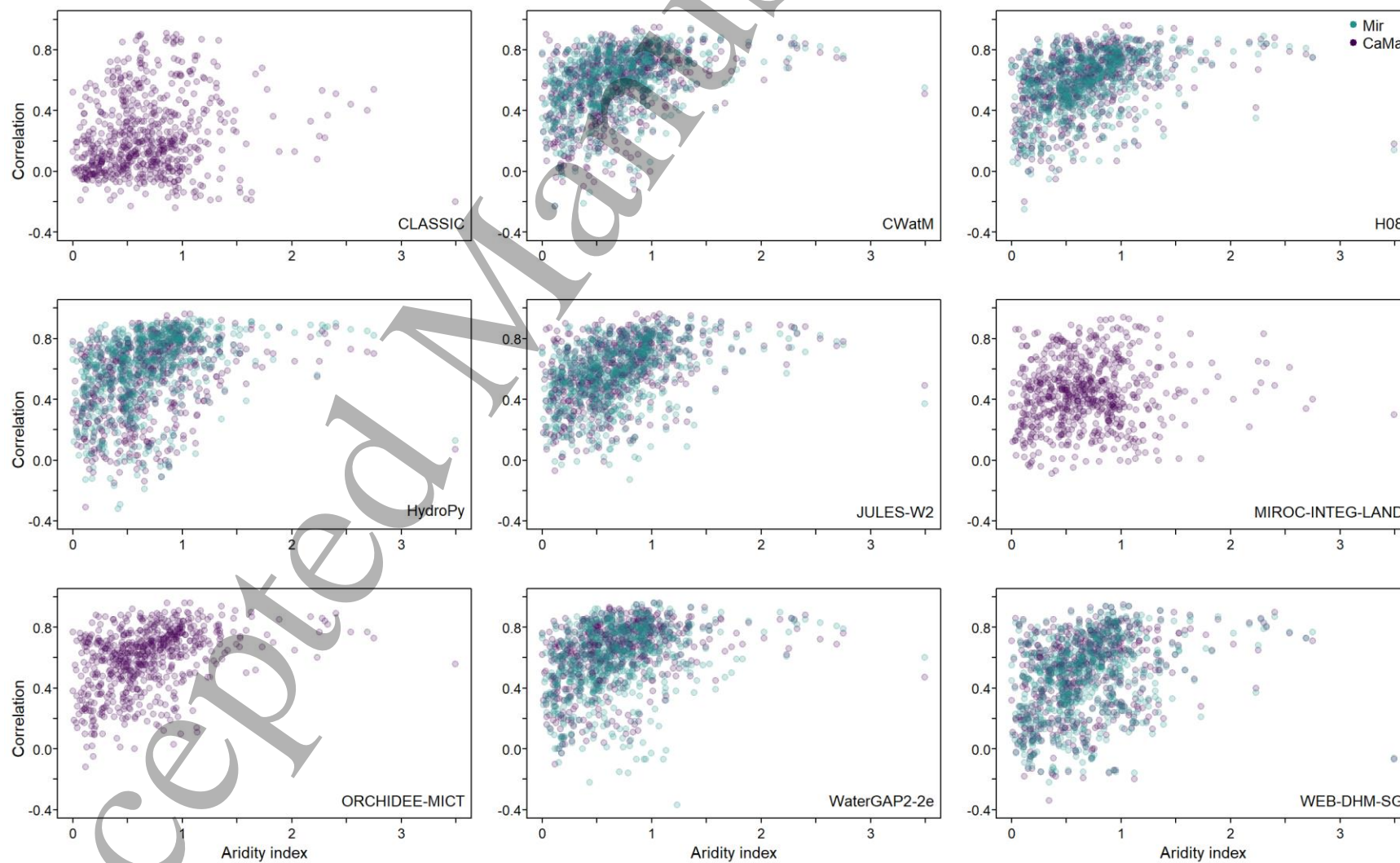


Figure 3. Relationship between aridity and model performance for daily discharge routed by the model's internal routing scheme (Mir) and CaMa-Flood (CaMa) across 644 stations. The aridity index is the ratio of precipitation to potential evapotranspiration (unitless, lower values correspond to more arid conditions, details in Zomer et al., 2022).

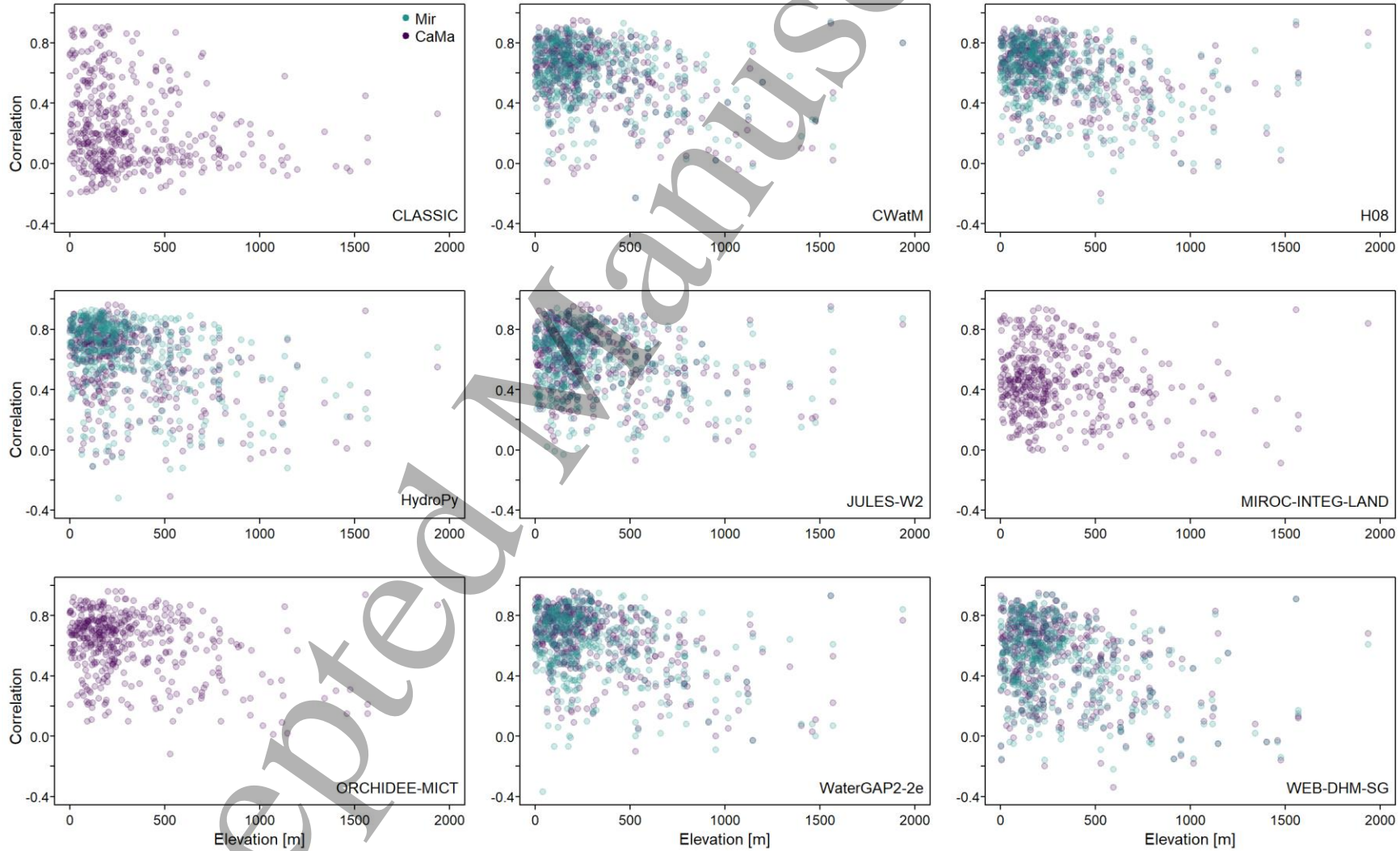


Figure 4. Relationship between mean catchment elevation and model performance for daily discharge routed by the model's internal routing scheme (Mir) and CaMa-Flood (CaMa) across 436 stations.

1
2
3
4
5
6
7
8
9
10
11
12
13
14
15
16
17
18
19
20
21
22
23
24
25
26
27
28
29
30
31
32
33
34
35
36
37
38
39
40
41
42
43
44
45
46
47

1
2
3 variability are more strongly overestimated (figure 2c, 2d). In contrast, for HydroPy and to a lesser extent
4 also for CWatM, discharge routed with CaMa-Flood tends to be worse compared to the model's internal
5 routing scheme (figure 2a), likely because variability is overestimated (figure 2d). For CWatM, HydroPy,
6 and JULES-W2, CaMa seems to particularly overestimate variability at higher elevations and steeper slopes
7 (table S7).
8
9
10
11
12

13 14 15 *3.2 Low flow*

16 Most models (six out of nine) do not capture the strength of low flow events, i.e., their magnitude of low
17 flow is simulated too high (figure 5, S9, S10). However, HydroPy and JULES-W2 are often close to
18 observed low flow, while WEB-DHM-SG tends to underestimate low flow (figure S9). Consistent with the
19 above results, low flow is overestimated in arid regions, especially in the Australian and African basins
20 (figure 5, S10). The exception is WEB-DHM-SG, which tends to underestimate low flow in these regions
21 as well.
22
23
24
25
26
27
28

29
30
31
32
33
34
35
36
37
38
39
40
41
42
43
44
45
46
47
48
49
50
51
52
53
54
55
56
57
58
59
60

Model performance is often worse for maximum annual discharge compared to daily discharge (seven
of nine models, figure 6, S11, S12). The median KGE of annual maximum discharge across all stations
ranges from -0.94 for WEB-DHM-SG to 0.24 for WaterGAP2-2e (figure 6a, table S8), and median
correlation ranges from 0.31 for CLASSIC to 0.58 for WaterGAP2-2e (figure 6b, table S8). There is a
tendency to overestimation (six of nine models), and for five models, river routing with CaMa-Flood leads
to a stronger overestimation compared to the model's internal routing scheme (figure 6c, table S8). The
maximum annual discharge is more strongly overestimated at stations in dry areas (figure S13, table S11).
Spatial analysis shows that eight out of nine models have a low KGE for most African basins, but a high
KGE for most basins in Asia (figure 7, S14). At the same time, performance for the other regions is more
heterogeneous.

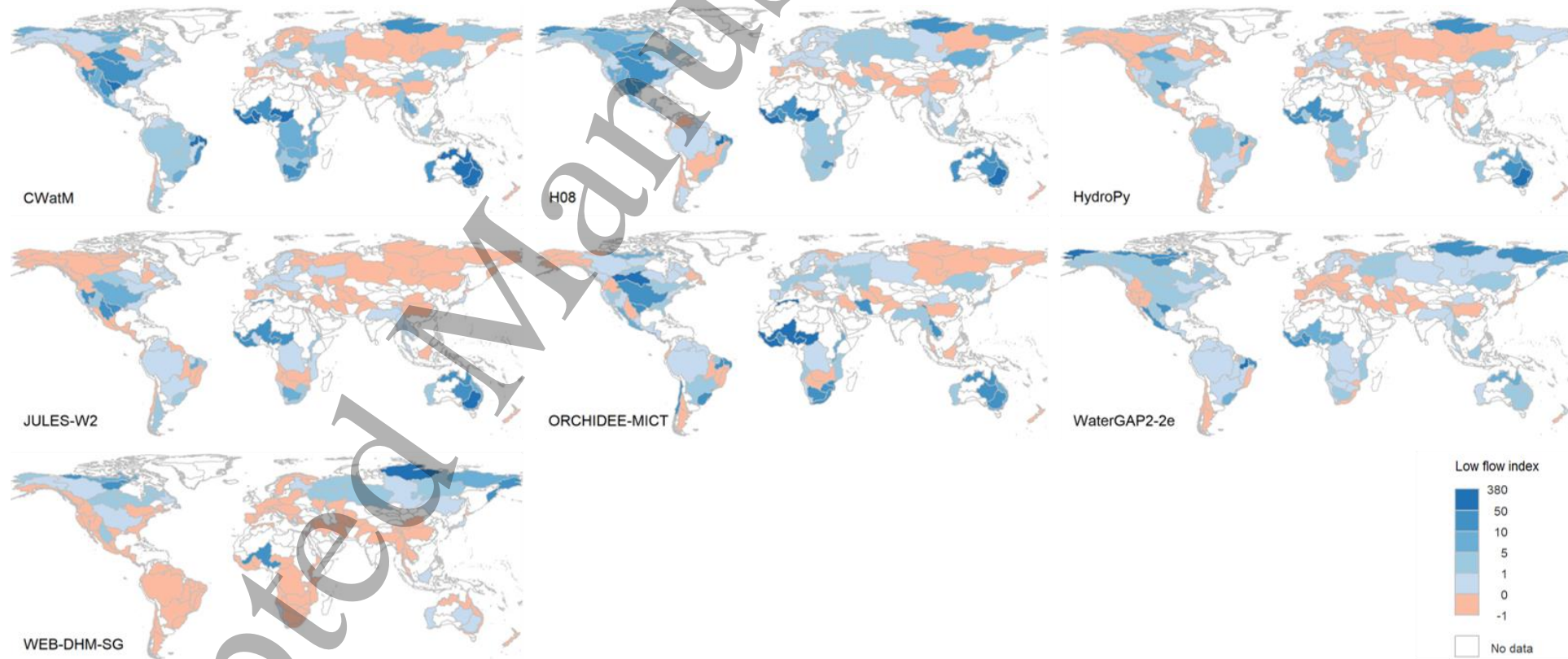


Figure 5. Low flow index (Q90) derived from daily discharge simulated by model's internal routing scheme, shown as basin average. Low flow index of zero implies perfect match between observation and simulation, negative values imply that low flow is simulated as too low, and positive values that low flow is simulated too high.

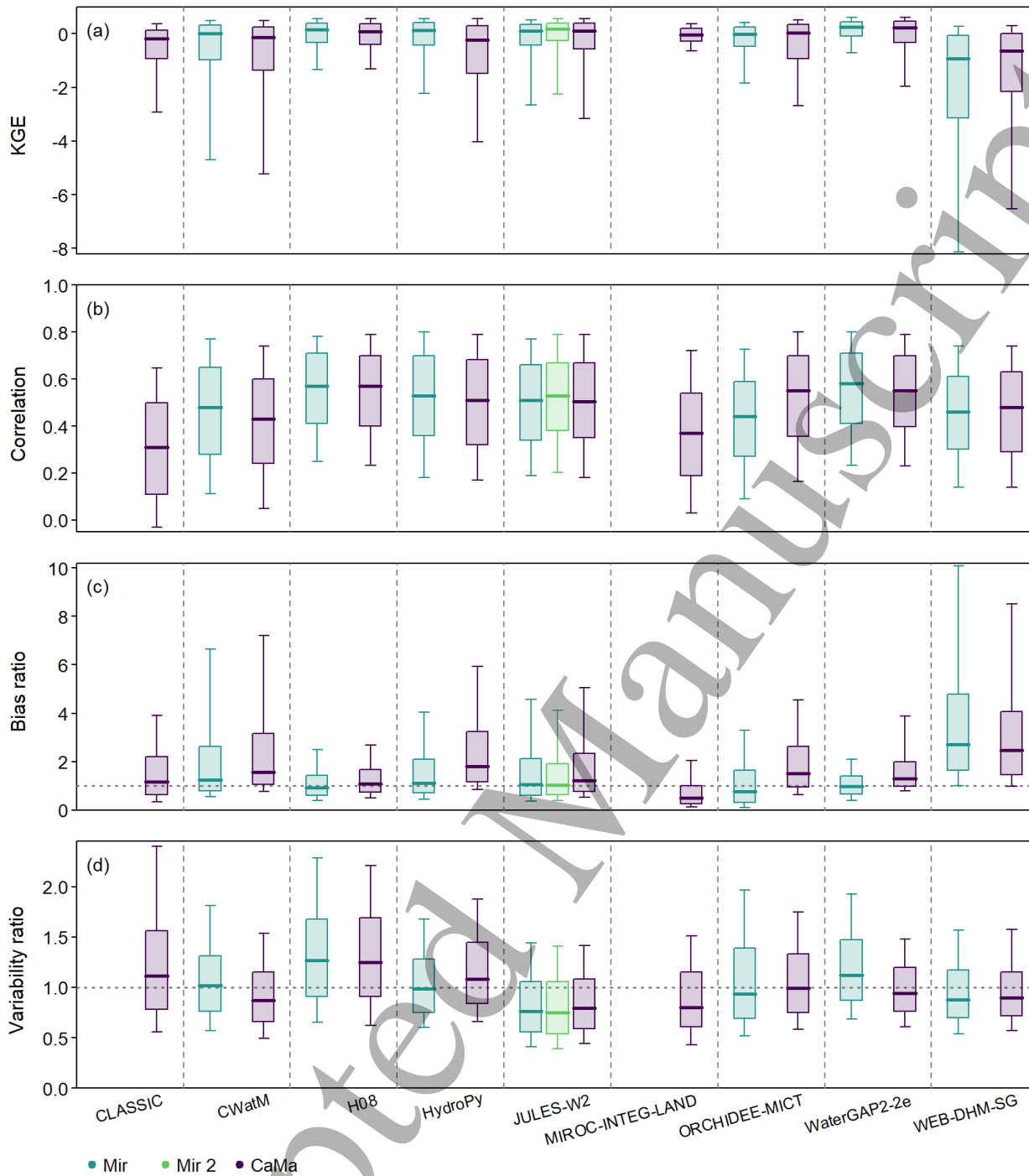


Figure 6. Evaluation of maximum annual discharge routed by the model's internal routing scheme (Mir) and CaMa-Flood (CaMa) across 644 stations for Kling-Gupta efficiency (KGE) and its three components. JULES-W2 provides discharge routed with two routing schemes (Mir, Mir2, details in table S1). Thick lines: median, box: first quartile and third quartile, whiskers: 10th and 90th percentile. Details table S8.

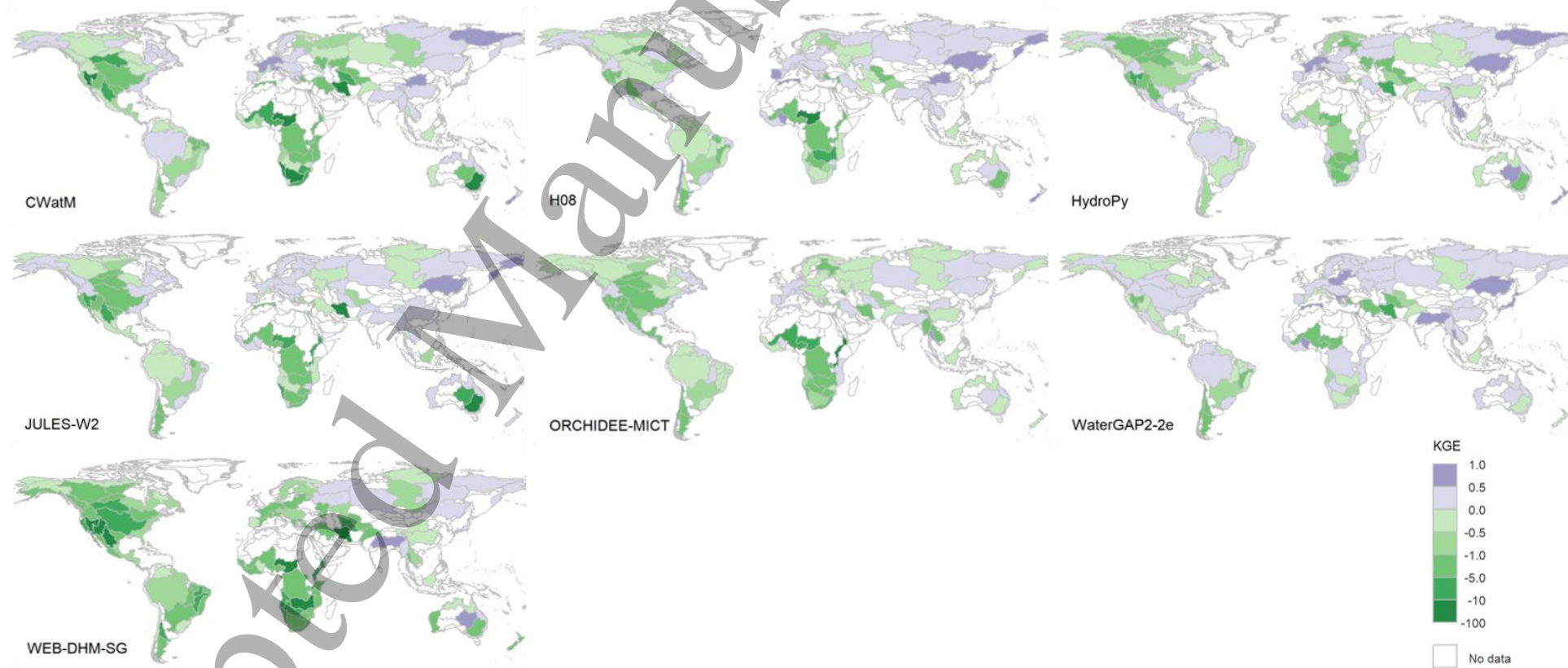


Figure 7. Kling-Gupta efficiency (KGE) for maximum annual discharge simulated by model's internal routing scheme, shown as basin average.

The analysis of which part of the distribution of annual maxima is over- or underestimated shows that five models (of nine) overestimate low and high maximum discharge (figure 8). Except for MIROC-INTEG-LAND, discharge routed with CaMa-Flood tends towards a stronger overestimation when compared to the model's internal routing scheme. There are some cases where models overestimate low values of annual maximum discharge and underestimate high values. In those cases, the average correlation between observed and simulated discharge is around 0.5. There are only individual stations where models consistently overestimate low values of annual maxima and underestimate high values (example in figure S15, S16).

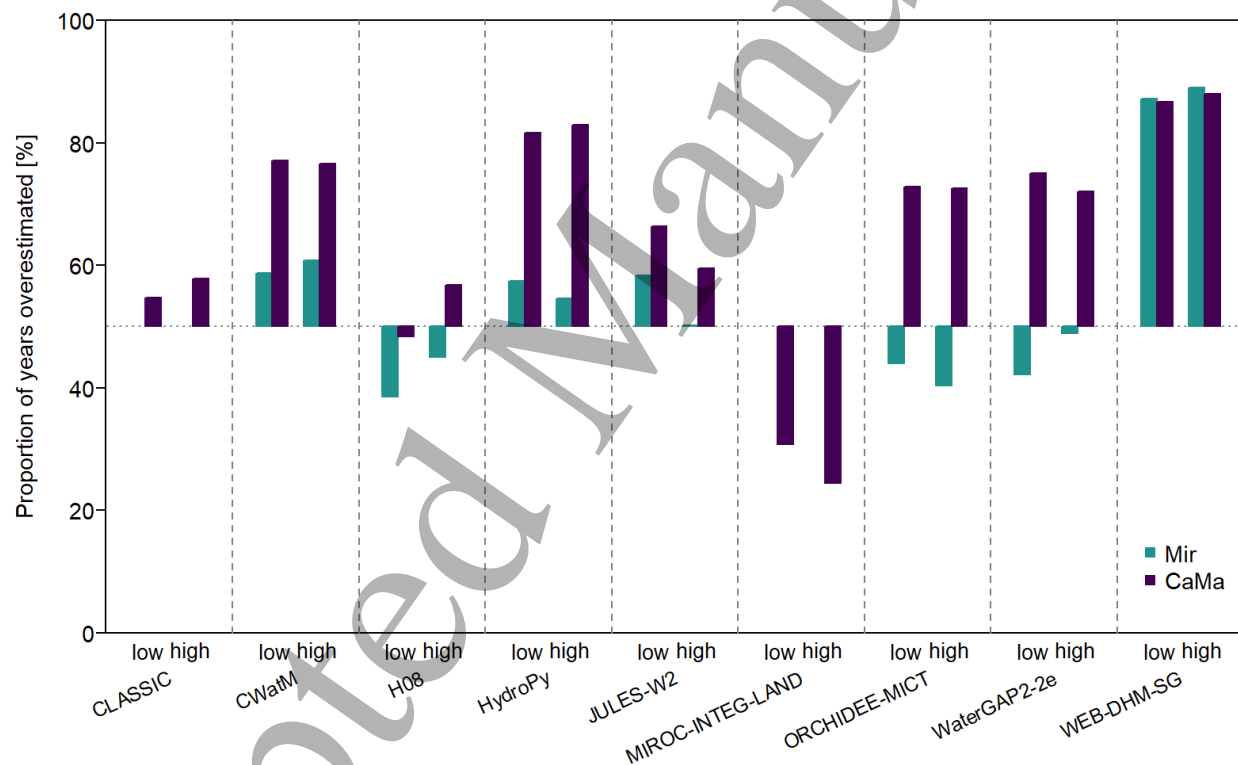


Figure 8. Proportion of years for which the annual maximum is overestimated for years with low annual maximum (years for which the annual maximum is below the observed median across the entire time series) and high annual maximum (years for which maximum is above median). Bars above the horizontal line at 50% show that the respective model tends towards overestimation.

3.4 Arid stations

Analysis of model performance across arid stations shows that all models perform better for mean monthly and mean annual discharge than for daily discharge due to a higher correlation coefficient (table

1
2
3 S13-S17, figure S17-S21). The correlation is highest for all models for long-term monthly discharge (table
4 S15, figure S19), suggesting that models can reproduce the seasonal flows.
5
6
7

8 **4 Discussion**

9
10 We demonstrate that in general, the evaluated models are able to reproduce observed time series of daily
11 and maximum annual discharge. The performance of ISIMIP3a models is similar to evaluation studies of
12 earlier simulation rounds. For example, Veldkamp *et al.* (2018) estimated for monthly discharge simulated
13 by ISIMIP2a models a median correlation of more than 0.6, and Hou *et al.* (2023) derived very similar
14 results for monthly runoff simulated by ISIMIP2a GHMs.
15
16
17
18
19

20
21 In line with previous studies (Veldkamp *et al.* 2018), the bias ratio is the evaluation parameter that
22 contributed most to a reduced performance in KGE. We find that most models overestimate discharge and
23 that the overestimation tends to be stronger for maximum annual discharge. For ISIMIP2a models,
24 Hattermann *et al.* (2017) also identified that models tend to overestimate monthly discharge, and similarly
25 Zaherpour *et al.* (2018) found that models overestimate extreme runoff. This suggests that applications
26 further down the modelling chain, for example, for flooded areas or flood damages could be affected as
27 well as other sectors such as agriculture or energy production. This is in line with a study showing that
28 simulations with some GHMs led to an overestimation of flooded areas (Mester *et al.* 2021).
29
30
31
32
33
34
35
36

37
38 Our further investigation of model performance for maximum annual discharge reveals that both low
39 and high values are either over- or underestimated (figure 8) as has been found by Zaherpour *et al.* (2018)
40 for ISIMIP2a models. Thus, contrary to the suggestion by Mester *et al.* (2021), we identify only a few cases
41 where a model overestimates low values and underestimates high values, i.e., a ‘too flat’ simulation. This
42 implies that we find no evidence for the proposal by Mester *et al.* (2021) that the flood return period by
43 GHMs is simulated too short.
44
45
46
47
48
49

50
51 Our evaluation setup of including seven GHMs with discharge routed by both, the model’s internal
52 routing scheme and CaMa-Flood, allows for investigating the role of the routing scheme. While Zhao *et al.*
53 (2017) detected that routing with CaMa-Flood led to a lower multi-year mean maximum discharge
54
55
56
57
58
59
60

(ISIMIP2a models), we here find that CaMa-Flood routing results in a higher proportion of years being overestimated for maximum annual discharge (figure 8). Also, except for WEB-DHM-SG, routing with CaMa-Flood has a higher bias ratio than the model's internal routing (figure 6c). Other studies found mixed performances for CaMa-Flood. Yang et al (2019) demonstrated that CaMa-Flood performs well for the amplitude of peak discharge but not the timing. In another study, the magnitude of 100-year floods was overestimated in Western and Central USA but underestimated in Eastern USA (Devitt *et al* 2021). However, in these studies, either CaMa-Flood was used as the only routing model (Yang *et al* 2019) or combinations of different GHMs, routing schemes, and climate forcing data were compared (Devitt *et al* 2021). Therefore, it is not clear which components of the modelling chain contribute errors. Our finding that CaMa-Flood tends to overestimate peak discharge, especially at higher elevations with steep slopes, suggests that too much water is transported in the river and floodplain during peak discharges. This may be explained by the fact that evapotranspiration over floodplains and transmission losses are not included in CaMa-Flood (Zhao *et al* 2017). In addition, routing by CaMa-Flood could be too efficient (i.e., water reaches a station too quickly), suggesting that flow velocity in the river channel or floodplain is overestimated. Unlike kinematic wave approaches, CaMa-Flood includes a diffusion term that allows the wave to spread spatially. While capturing the spatial variability of flow velocity within the channel, the diffusive wave equation tends to concentrate the flow more rapidly in the case of rapid changes in flow, e.g., due to sudden changes in channel slope or rapid increases in discharge. As a result, peak discharges may be overestimated, particularly in higher elevation areas. In addition, flow velocity is influenced by river channel and floodplain characteristics, some of which are derived empirically in CaMa-Flood. This leads to uncertainties and potential biases in the estimation of peak discharges (Yamazaki *et al* 2011).

When analysing which catchment properties are linked to model performance we find that two natural features, and not anthropogenic ones, are especially relevant. First, it is well established that hydrological models perform less well in arid and semi-arid regions (Zaherpour *et al* 2018, Hou *et al* 2023). We find that this is also the case for ISIMIP3a GHMs (figure 3). Dry areas have a low runoff coefficient meaning that a large proportion of the precipitation evaporates, and thus a small underestimation of evapotranspiration by

1
2
3 a model can lead to a strong overestimation of discharge (Hattermann *et al* 2017). As we find that discharge
4 is more strongly overestimated in arid areas compared to humid areas (figure S4), this could mean that
5 evapotranspiration may be underestimated particularly in arid areas. Given the relevance of hydrological
6 modelling for projecting climate change impacts on drought prevalence in (semi-) arid areas (Wang *et al*
7 2022), reducing bias in simulating discharge under dry conditions is an important area of future model
8 improvement. However, as we find that the models show a high correlation for long-term mean monthly
9 discharge, GHMs could be used to analyse changes in seasonal flows in (semi-) arid areas.

10
11
12
13
14
15
16
17
18 Second, we find that models perform less well at higher elevations, as has been shown for ISIMIP2a
19 (Yang *et al* 2019). This suggests that cold dynamics, i.e., glaciers, permafrost, and snowmelt, are important
20 hydrological processes that are not yet adequately included in many models and are thus a further relevant
21 area of model development (Gädeke *et al* 2020).

22
23
24
25
26 As the output of GHMs is used to answer a range of different research questions including the impact of
27 climate change on various aspects of the water cycle (Krysanova *et al* 2020), it is important to assess
28 additional hydrological variables. For example, there is ongoing work evaluating terrestrial water storage
29 and soil moisture simulated by GHMs from ISIMIP3a (Tiwari *et al* under review). A next step would be to
30 validate other GHM output variables, such as evapotranspiration and groundwater recharge, as has been
31 done in ISIMIP2 assessment studies (Gnann *et al* 2023, Wartenburger *et al* 2018, Pokhrel *et al* 2021).

32
33
34
35
36
37
38
39 We conclude that our results help to identify areas where we have greater confidence in the ability of
40 GHMs to simulate hydrological processes, particularly in humid areas, at low elevations and in areas with
41 strong and regular seasonality. Stations in these areas are therefore likely to be best suited to studies aimed
42 at attributing historical climate change based on the output of the investigated GHMs. We also identify
43 areas where improved process simulation is needed, i.e., evapotranspiration, transmission losses and cold
44 dynamics.

45
46
47
48
49
50
51
52
53
54
55
56
57
58
59
60
Accepted Manuscript

Acknowledgements

This research has received funding from the German Federal Ministry of Education and Research (BMBF) under the research projects QUIDIC (01LP1907A) and ISIAccess (16QK05), and is based upon work from COST Action CA19139 PROCLIAS (PROcess-based models for CLimate Impact Attribution across Sectors), supported by COST (European Cooperation in Science and Technology; <https://www.cost.eu>).

References

- Best M J, Pryor M, Clark D B, Rooney G G, Essery R L H, Ménard C B, Edwards J M, Hendry M A, Porson A, Gedney N, Mercado L M, Sitch S, Blyth E, Boucher O, Cox P M, Grimmond C S B and Harding R J 2011 The Joint UK Land Environment Simulator (JULES), model description – Part 1: Energy and water fluxes *Geoscientific Model Development* **4** 677–99
- Boulangé J, Yoshida T, Nishina K, Okada M and Hanasaki N 2023 Delivering the latest global water resource simulation results to the public *Climate Services* **30** 100386
- Burek P, Satoh Y, Kahil T, Tang T, Greve P, Smilovic M, Guillaumot L, Zhao F and Wada Y 2020 Development of the Community Water Model (CWatM v1.04) – a high-resolution hydrological model for global and regional assessment of integrated water resources management *Geoscientific Model Development* **13** 3267–98
- Dankers R, Arnell N W, Clark D B, Falloon P D, Fekete B M, Gosling S N, Heinke J, Kim H, Masaki Y, Satoh Y, Stacke T, Wada Y and Wisser D 2014 First look at changes in flood hazard in the Inter-Sectoral Impact Model Intercomparison Project ensemble *Proceedings of the National Academy of Sciences* **111** 3257–61
- Devitt L, Neal J, Wagener T and Coxon G 2021 Uncertainty in the extreme flood magnitude estimates of large-scale flood hazard models *Environ. Res. Lett.* **16** 064013
- Do H X, Gudmundsson L, Leonard M and Westra S 2018 The Global Streamflow Indices and Metadata Archive (GSIM) – Part 1: The production of a daily streamflow archive and metadata *Earth System Science Data* **10** 765–85
- Frieler K, Volkholz J, Lange S, Schewe J, Mengel M, del Rocío Rivas López M, Otto C, Reyer C P O, Karger D N, Malle J T, Treu S, Menz C, Blanchard J L, Harrison C S, Petrik C M, Eddy T D, Ortega-Cisneros K, Novaglio C, Rousseau Y, Watson R A, Stock C, Liu X, Heneghan R, Tittensor D, Maury O, Büchner M, Vogt T, Wang T, Sun F, Sauer I J, Koch J, Vanderkelen I, Jägermeyr J, Müller C, Rabin S, Klar J, Vega del Valle I D, Lasslop G, Chadburn S, Burke E, Gallego-Sala A, Smith N, Chang J, Hantson S, Burton C, Gädeke A, Li F, Gosling S N, Müller Schmied H, Hattermann F, Wang J, Yao F, Hickler T, Marcé R, Pierson D, Thiery W, Mercado-Bettín D, Ladwig R, Ayala-Zamora A I, Forrest M and Bechtold M 2024 Scenario setup and forcing data for impact model evaluation and impact attribution within the third round of the Inter-Sectoral Model Intercomparison Project (ISIMIP3a) *Geoscientific Model Development* **17** 1–51

- 1
2
3 Gädeke A, Krysanova V, Aryal A, Chang J, Grillakis M, Hanasaki N, Koutroulis A, Pokhrel Y, Satoh Y,
4 Schaphoff S, Müller Schmied H, Stacke T, Tang Q, Wada Y and Thonicke K 2020 Performance
5 evaluation of global hydrological models in six large Pan-Arctic watersheds *Climatic Change* **163**
6 1329–51
7
- 8
9 Gnann S, Reinecke R, Stein L, Wada Y, Thiery W, Müller Schmied H, Satoh Y, Pokhrel Y, Ostberg S,
10 Koutroulis A, Hanasaki N, Grillakis M, Gosling S N, Burek P, Bierkens M F P and Wagener T 2023
11 Functional relationships reveal differences in the water cycle representation of global water
12 models *Nat Water* **1** 1079–90
13
- 14 Gosling S N, Zaherpour J, Mount N J, Hattermann F F, Dankers R, Arheimer B, Breuer L, Ding J, Haddeland
15 I, Kumar R, Kundu D, Liu J, van Griensven A, Veldkamp T I E, Vetter T, Wang X and Zhang X 2017 A
16 comparison of changes in river runoff from multiple global and catchment-scale hydrological
17 models under global warming scenarios of 1 °C, 2 °C and 3 °C *Climatic Change* **141** 577–95
18
- 19 Gudmundsson L, Boulange J, Do H X, Gosling S N, Grillakis M G, Koutroulis A G, Leonard M, Liu J, Müller
20 Schmied H, Papadimitriou L, Pokhrel Y, Seneviratne S I, Satoh Y, Thiery W, Westra S, Zhang X and
21 Zhao F 2021 Globally observed trends in mean and extreme river flow attributed to climate
22 change *Science* **371** 1159–62
23
- 24 Gudmundsson L, Do H X, Leonard M and Westra S 2018 The Global Streamflow Indices and Metadata
25 Archive (GSIM) – Part 2: Quality control, time-series indices and homogeneity assessment *Earth*
26 *System Science Data* **10** 787–804
27
- 28 Guimberteau M, Zhu D, Maignan F, Huang Y, Yue C, Dantec-Nédélec S, Otlé C, Jornet-Puig A, Bastos A,
29 Laurent P, Goll D, Bowring S, Chang J, Guenet B, Tifafi M, Peng S, Krinner G, Ducharne A, Wang F,
30 Wang T, Wang X, Wang Y, Yin Z, Lauerwald R, Joetzjer E, Qiu C, Kim H and Ciais P 2018 ORCHIDEE-
31 MICT (v8.4.1), a land surface model for the high latitudes: model description and validation
32 *Geoscientific Model Development* **11** 121–63
33
- 34 Hallegatte S, Vogt-Schilb A, Bangalore M and Rozenberg J 2017 *Unbreakable: Building the Resilience of the*
35 *Poor in the Face of Natural Disasters* (Washington, DC: World Bank) Online:
36 <http://hdl.handle.net/10986/25335>
37
- 38 Hattermann F F, Krysanova V, Gosling S N, Dankers R, Daggupati P, Donnelly C, Flörke M, Huang S,
39 Motovilov Y, Buda S, Yang T, Müller C, Leng G, Tang Q, Portmann F T, Hagemann S, Gerten D,
40 Wada Y, Masaki Y, Alemayehu T, Satoh Y and Samaniego L 2017 Cross-scale intercomparison of
41 climate change impacts simulated by regional and global hydrological models in eleven large river
42 basins *Climatic Change* **141** 561–76
43
- 44 Hirabayashi Y, Tanoue M, Sasaki O, Zhou X and Yamazaki D 2021 Global exposure to flooding from the
45 new CMIP6 climate model projections *Sci Rep* **11** 3740
46
- 47 Hou Y, Guo H, Yang Y and Liu W 2023 Global Evaluation of Runoff Simulation From Climate, Hydrological
48 and Land Surface Models *Water Resources Research* **59** e2021WR031817
49
- 50 Kling H, Fuchs M and Paulin M 2012 Runoff conditions in the upper Danube basin under an ensemble of
51 climate change scenarios *Journal of Hydrology* **424–425** 264–77
52
53
54
55
56
57
58
59
60

- 1
2
3 Knoben W J M, Freer J E and Woods R A 2019 Technical note: Inherent benchmark or not? Comparing
4 Nash–Sutcliffe and Kling–Gupta efficiency scores *Hydrology and Earth System Sciences* **23** 4323–
5 31
6
7 Kryanova V, Hattermann F F and Kundzewicz Z W 2020 How evaluation of hydrological models influences
8 results of climate impact assessment—an editorial *Climatic Change* **163** 1121–41
9
10 Kryanova V, Vetter T, Eisner S, Huang S, Pechlivanidis I, Strauch M, Gelfan A, Kumar R, Aich V, Arheimer
11 B, Chamorro A, Griensven A van, Kundu D, Lobanova A, Mishra V, Plötner S, Reinhardt J, Seidou
12 O, Wang X, Wortmann M, Zeng X and Hattermann F F 2017 Intercomparison of regional-scale
13 hydrological models and climate change impacts projected for 12 large river basins worldwide—
14 a synthesis *Environ. Res. Lett.* **12** 105002
15
16
17 Kumar A, Gosling S N, Johnson M F, Jones M D, Zaherpour J, Kumar R, Leng G, Schmied H M, Kupzig J,
18 Breuer L, Hanasaki N, Tang Q, Ostberg S, Stacke T, Pokhrel Y, Wada Y and Masaki Y 2022 Multi-
19 model evaluation of catchment- and global-scale hydrological model simulations of drought
20 characteristics across eight large river catchments *Advances in Water Resources* **165** 104212
21
22
23 Lange S, Mengel M, Treu S and Büchner M 2023 ISIMIP3a atmospheric climate input data (v1.2). ISIMIP
24 Repository. *ISIMIP Repository*
25
26 Lange S, Menz C, Gleixner S, Cucchi M, Weedon G P, Amici A, Bellouin N, Müller Schmied H, Hersbach H,
27 Buontempo C and Cagnazzo C 2021 WFDE5 over land merged with ERA5 over the ocean (W5E5
28 v2.0) *ISIMIP Repository* Online: <https://data.isimip.org/10.48364/data.isimip.org>
29
30 Lange S, Volkholz J, Geiger T, Zhao F, Vega I, Veldkamp T, Reyer C P O, Warszawski L, Huber V, Jägermeyr
31 J, Schewe J, Bresch D N, Büchner M, Chang J, Ciais P, Dury M, Emanuel K, Folberth C, Gerten D,
32 Gosling S N, Grillakis M, Hanasaki N, Henrot A-J, Hickler T, Honda Y, Ito A, Khabarov N, Koutroulis
33 A, Liu W, Müller C, Nishina K, Ostberg S, Müller Schmied H, Seneviratne S I, Stacke T, Steinkamp J,
34 Thiery W, Wada Y, Willner S, Yang H, Yoshikawa M, Yue C and Frieler K 2020 Projecting Exposure
35 to Extreme Climate Impact Events Across Six Event Categories and Three Spatial Scales *Earth's*
36 *Future* **8** e2020EF001616
37
38
39 Lehner B and Grill G 2013 Global river hydrography and network routing: baseline data and new
40 approaches to study the world's large river systems *Hydrological Processes* **27** 2171–86
41
42 Liu J, Yang H, Gosling S N, Kumm M, Flörke M, Pfister S, Hanasaki N, Wada Y, Zhang X, Zheng C, Alcamo J
43 and Oki T 2017a Water scarcity assessments in the past, present, and future *Earth's Future* **5** 545–
44 59
45
46
47 Liu X, Tang Q, Cui H, Mu M, Gerten D, Gosling S N, Masaki Y, Satoh Y and Wada Y 2017b Multimodel
48 uncertainty changes in simulated river flows induced by human impact parameterizations *Environ.*
49 *Res. Lett.* **12** 025009
50
51 Maxwell S L, Butt N, Maron M, McAlpine C A, Chapman S, Ullmann A, Segan D B and Watson J E M 2019
52 Conservation implications of ecological responses to extreme weather and climate events
53 *Diversity and Distributions* **25** 613–25
54
55
56
57
58
59
60

- 1
2
3 Melton J R, Arora V K, Wisernig-Cojoc E, Seiler C, Fortier M, Chan E and Teckentrup L 2020 CLASSIC v1.0:
4 the open-source community successor to the Canadian Land Surface Scheme (CLASS) and the
5 Canadian Terrestrial Ecosystem Model (CTEM) – Part 1: Model framework and site-level
6 performance *Geoscientific Model Development* **13** 2825–50
7
- 8 Mester B, Willner S N, Frieler K and Schewe J 2021 Evaluation of river flood extent simulated with multiple
9 global hydrological models and climate forcings *Environ. Res. Lett.* **16** 094010
10
- 11 Müller Schmied H, Cáceres D, Eisner S, Flörke M, Herbert C, Niemann C, Peiris T A, Popat E, Portmann F T,
12 Reinecke R, Schumacher M, Shadkam S, Telteu C-E, Trautmann T and Döll P 2021 The global water
13 resources and use model WaterGAP v2.2d: model description and evaluation *Geoscientific Model
14 Development* **14** 1037–79
15
- 16 Müller Schmied H and Schiebener L 2022 *Assessing the suitability of streamflow station observations for
17 consistent evaluation of simulated river discharge data of the ISIMIP global water sector
18 (Frankfurt, Germany: PROCLIAS)*
19
- 20 Müller Schmied H, Trautmann T, Ackermann S, Cáceres D, Flörke M, Gerdener H, Kynast E, Peiris T A,
21 Schiebener L, Schumacher M and Döll P 2023 The global water resources and use model
22 WaterGAP v2.2e: description and evaluation of modifications and new features *Geoscientific
23 Model Development Discussions* 1–46
24
- 25 Munich Re 2016 *NatCatSERVICE Database*
26
- 27 Pokhrel Y, Felfelani F, Satoh Y, Boulange J, Burek P, Gädeke A, Gerten D, Gosling S N, Grillakis M,
28 Gudmundsson L, Hanasaki N, Kim H, Koutroulis A, Liu J, Papadimitriou L, Schewe J, Müller Schmied
29 H, Stacke T, Telteu C-E, Thiery W, Veldkamp T, Zhao F and Wada Y 2021 Global terrestrial water
30 storage and drought severity under climate change *Nat. Clim. Chang.* **11** 226–33
31
- 32 Qi W, Feng L, Yang H, Liu J, Zheng Y, Shi H, Wang L and Chen D 2022 Economic growth dominates rising
33 potential flood risk in the Yangtze River and benefits of raising dikes from 1991 to 2015 *Environ.
34 Res. Lett.* **17** 034046
35
- 36 Sauer I J, Reese R, Otto C, Geiger T, Willner S N, Guillod B P, Bresch D N and Frieler K 2021 Climate signals
37 in river flood damages emerge under sound regional disaggregation *Nat Commun* **12** 2128
38
- 39 Schewe J, Heinke J, Gerten D, Haddeland I, Arnell N W, Clark D B, Dankers R, Eisner S, Fekete B M, Colón-
40 González F J, Gosling S N, Kim H, Liu X, Masaki Y, Portmann F T, Satoh Y, Stacke T, Tang Q, Wada
41 Y, Wisser D, Albrecht T, Frieler K, Piontek F, Warszawski L and Kabat P 2014 Multimodel
42 assessment of water scarcity under climate change *Proceedings of the National Academy of
43 Sciences* **111** 3245–50
44
- 45 Stacke T and Hagemann S 2021 HydroPy (v1.0): a new global hydrology model written in Python
46 *Geoscientific Model Development* **14** 7795–816
47
- 48 Thompson J R, Gosling S N, Zaherpour J and Laizé C L R 2021 Increasing Risk of Ecological Change to Major
49 Rivers of the World With Global Warming *Earth's Future* **9** e2021EF002048
50
51
52
53
54
55
56
57
58
59
60

- 1
2
3 Tiwari A D, Pokhrel Y, Boulange J, Burek P, Guillaumot L, Gosling S N, Grillakis M, Hanasaki N, Koutroulis
4 A, Otta K, Müller Schmied H, Satoh Y, Scanlon B, Sebastian O, Stacke T and Yokohata T under
5 review Similarities and divergent patterns in hydrologic fluxes and storages simulated by global
6 water models *Nature Water*
- 7
8
9 Tsilimigkras A, Clark D B, Hartley A J, Burke E J, Grillakis M G and Koutroulis A G under review Spatially-
10 varying parametrization of the Total Runoff Integrating Pathways (TRIP) scheme for improved
11 river routing at the global scale *Advances in Water Resources*
- 12
13 Tsilimigkras A, Clark D, Hartley A, Burke E, Grillakis M and Koutroulis A 2023 Using basin-scale
14 physiographic attributes to improve river routing in JULES *EGU General Assembly Conference*
15 *Abstracts EGU23* Online: <https://meetingorganizer.copernicus.org/EGU23/EGU23-14079.html>
- 16
17 Van Vliet M T H 2023 Complex interplay of water quality and water use affects water scarcity under
18 droughts and heatwaves *Nat Water* **1** 902–4
- 19
20
21 Veldkamp T I E, Zhao F, Ward P J, Moel H de, Aerts J C J H, Schmied H M, Portmann F T, Masaki Y, Pokhrel
22 Y, Liu X, Satoh Y, Gerten D, Gosling S N, Zaherpour J and Wada Y 2018 Human impact
23 parameterizations in global hydrological models improve estimates of monthly discharges and
24 hydrological extremes: a multi-model validation study *Environ. Res. Lett.* **13** 055008
- 25
26 Wang Z, Yang Y, Zhang C, Guo H and Hou Y 2022 Historical and future Palmer Drought Severity Index with
27 improved hydrological modeling *Journal of Hydrology* **610** 127941
- 28
29 Wartenburger R, Seneviratne S I, Hirschi M, Chang J, Ciais P, Deryng D, Elliott J, Folberth C, Gosling S N,
30 Gudmundsson L, Henrot A-J, Hickler T, Ito A, Khabarov N, Kim H, Leng G, Liu J, Liu X, Masaki Y,
31 Morfopoulos C, Müller C, Schmied H M, Nishina K, Orth R, Pokhrel Y, Pugh T A M, Satoh Y,
32 Schaphoff S, Schmid E, Sheffield J, Stacke T, Steinkamp J, Tang Q, Thiery W, Wada Y, Wang X,
33 Weedon G P, Yang H and Zhou T 2018 Evapotranspiration simulations in ISIMIP2a—Evaluation of
34 spatio-temporal characteristics with a comprehensive ensemble of independent datasets *Environ.*
35 *Res. Lett.* **13** 075001
- 36
37
38 Yamazaki D, Kanae S, Kim H and Oki T 2011 A physically based description of floodplain inundation
39 dynamics in a global river routing model *Water Resources Research* **47** Online:
40 <https://onlinelibrary.wiley.com/doi/abs/10.1029/2010WR009726>
- 41
42 Yang T, Sun F, Gentile P, Liu W, Wang H, Yin J, Du M and Liu C 2019 Evaluation and machine learning
43 improvement of global hydrological model-based flood simulations *Environ. Res. Lett.* **14** 114027
- 44
45 Yokohata T, Kinoshita T, Sakurai G, Pokhrel Y, Ito A, Okada M, Satoh Y, Kato E, Nitta T, Fujimori S, Felfelani
46 F, Masaki Y, Iizumi T, Nishimori M, Hanasaki N, Takahashi K, Yamagata Y and Emori S 2020 MIROC-
47 INTEG-LAND version 1: a global biogeochemical land surface model with human water
48 management, crop growth, and land-use change *Geoscientific Model Development* **13** 4713–47
- 49
50
51 Yoshida T, Hanasaki N, Nishina K, Boulange J, Okada M and Troch P A 2022 Inference of Parameters for a
52 Global Hydrological Model: Identifiability and Predictive Uncertainties of Climate-Based
53 Parameters *Water Resources Research* **58** e2021WR030660
- 54
55
56
57
58
59
60

1
2
3 Zaherpour J, Gosling S N, Mount N, Schmied H M, Veldkamp T I E, Dankers R, Eisner S, Gerten D,
4 Gudmundsson L, Haddeland I, Hanasaki N, Kim H, Leng G, Liu J, Masaki Y, Oki T, Pokhrel Y, Satoh
5 Y, Schewe J and Wada Y 2018 Worldwide evaluation of mean and extreme runoff from six global-
6 scale hydrological models that account for human impacts *Environ. Res. Lett.* **13** 065015
7

8
9 Zhao F, Veldkamp T I E, Frieler K, Schewe J, Ostberg S, Willner S, Schauburger B, Gosling S N, Schmied H
10 M, Portmann F T, Leng G, Huang M, Liu X, Tang Q, Hanasaki N, Biemans H, Gerten D, Satoh Y,
11 Pokhrel Y, Stacke T, Ciais P, Chang J, Ducharne A, Guimberteau M, Wada Y, Kim H and Yamazaki D
12 2017 The critical role of the routing scheme in simulating peak river discharge in global
13 hydrological models *Environ. Res. Lett.* **12** 075003
14

15 Zomer R J, Xu J and Trabucco A 2022 Version 3 of the Global Aridity Index and Potential Evapotranspiration
16 Database *Sci Data* **9** 409
17
18
19
20
21
22
23
24
25
26
27
28
29
30
31
32
33
34
35
36
37
38
39
40
41
42
43
44
45
46
47
48
49
50
51
52
53
54
55
56
57
58
59
60